

# The X-ray measurements of the supermirror using synchrotron radiation

T. Okajima, S. Ichimaru, K. Tamura, K. Haga, Y. Ogasaka, S. Takahashi,  
S. Fukuda, H. Kitou, A. Gotou, Y. Tawara, K. Yamashita,  
Y. Tsusaka<sup>a</sup>, S. Takeda<sup>a</sup> and H. Kunieda<sup>b</sup>

*Dept. of Physics, Nagoya University, Nagoya, Japan*

*<sup>a</sup>Himeji Institute of Technology, Hyogo, Japan*

*<sup>b</sup>The Institute of Space and Astronautical Science, Sagami, Japan*

## ABSTRACT

We measured Pt/C multilayers and supermirrors with hard X-rays at synchrotron radiation facility SPring-8. These mirrors were fabricated for the hard X-ray telescope on board our balloon-borne experiment named InFOC $\mu$ S. The energy band of InFOC $\mu$ S telescope is from 20 to 40 keV, thus characterization of reflectors with hard X-rays above 20 keV is important. SPring-8 is one of the world's most powerful third-generation synchrotron radiation facility. We measured multilayers and several types of supermirrors. We also measured reflectivity of supermirrors on three different kind of substrates; float glass, gold replica foil and platinum replica foil. From the reflectivity measurements, performance of these supermirrors was found quite satisfactory for our telescope. Furthermore platinum replica foil substrate showed significantly better reflectivity than gold replica foil. Thus we chose platinum replica foil as a substrate for flight reflectors. Scattering measurements gave us important informations. Our preliminary analysis showed that the scattered power distribution can be explained as a convolution of structures in lateral and depth direction.

**Keywords:** multilayer, supermirror, hard x-ray optics, x-ray scattering

## 1. INTRODUCTION

The principle of X-ray reflection by ordinary X-ray mirrors is a total external reflection by single layer of metal. Typical high energy limit is around 10 keV at grazing incidence angles of around 0.5 degrees. Above the critical energy, X-rays start to penetrate into material and can be reflected by the interference of periodic structures like crystal lattice or multilayers. Multilayer has an advantage to enhance reflectivity beyond the critical energy. However its energy bandwidth is usually narrow under the constraint of the Bragg condition. In the case of application to X-ray telescope, wide energy band path is preferred. To broaden the energy band, multilayer with graded periodic length into depth direction, so called supermirror, is known to be promising.

We have developed hard X-ray reflector using supermirrors of platinum-carbon combination, especially for astronomical application. So far, we have succeeded to make demonstrational model of hard X-ray telescope and to show its imaging capability. The telescope consists of 10 pairs of conical foil mirror shells whose surfaces are coated with platinum-carbon supermirrors. The detail of the experiment is summarized by Yamashita *et al.* (1998a). Following to the demonstrational experiment, we have started to make reflectors for balloon borne hard X-ray telescope mission named InFOC $\mu$ S (International Focusing Optics Collaboration for  $\mu$ Crab Sensitivity).

The focus of this paper is on the characterization of supermirrors, in particular, those for InFOC $\mu$ S telescope. In the previous papers (see e.g. Tamura *et al.*, 1997), we have reported on the measurement at 8.04 keV (Cu-K $\alpha$ ) and 17.4 keV (Mo-K $\alpha$ ) using conventional X-ray source. However, the performance of our supermirrors in hard X-ray region is still not fully understood. Since our supermirrors are designed for application to hard X-ray region above 10 keV, it is important to know their performance in this energy region. Also, measurement at higher energies, where penetration length is longer, has advantages to study layer structures down to deepest layers. For example, largest number of layer pairs in our design is 60 and total thickness of heavy element (platinum) is about 54 nm, where X-rays below about 40 keV has insufficient penetration power. For these purposes, we carried out a series of hard X-ray measurements at high brilliance synchrotron facility, SPring-8. In this paper, we report the result of reflectivity and scattering measurement in hard X-rays.

---

Takashi Okajima: E-mail: okajima@u.phys.nagoya-u.ac.jp

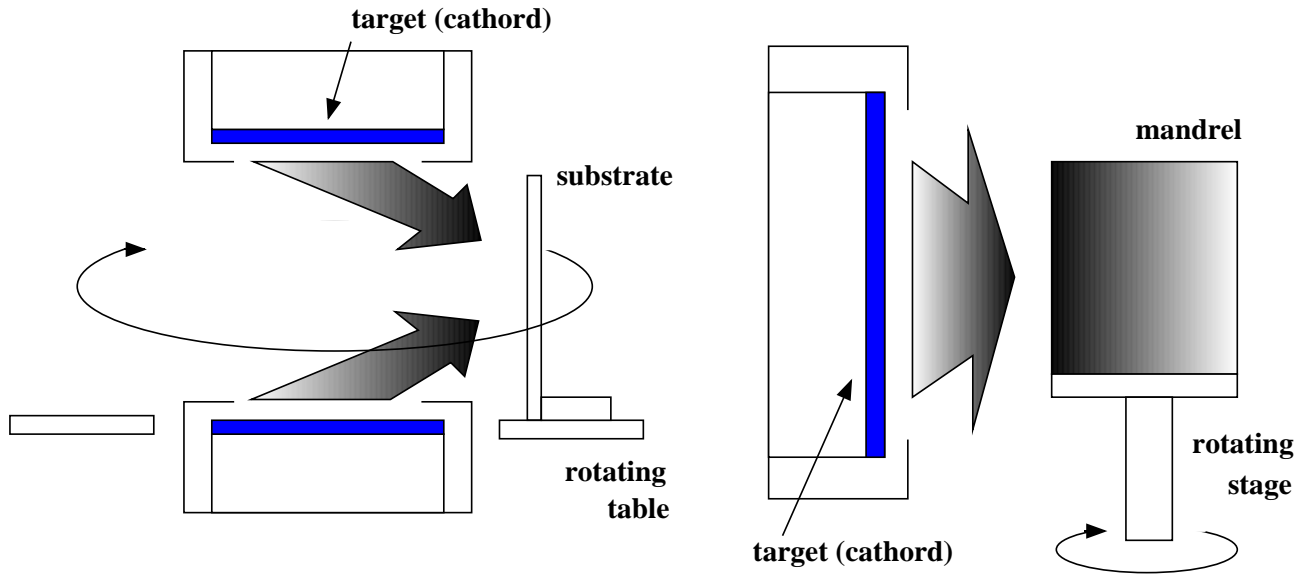


**Figure 1.** Schematics of the DC magnetron sputtering system. Left figure shows the sputtering system for deposition onto platinum replica foil. The target is facing to each other and the substrate rotates around the target. Right figure shows the sputtering system for deposition onto a mandrel. The target is facing to the mandrel and the mandrel rotates itself.

## 2. DESIGN AND FABRICATION OF SUPERMIRRORS

We, Nagoya group and X- and  $\gamma$ -ray groups at NASA/Goddard Space Flight Center(GSFC) agreed to perform the international balloon project for the focusing telescopes in hard X-ray range. It is named “InFOC $\mu$ S”. The basic plan is the combination of the high throughput X-ray telescope equipped supermirror on reflectors and the hard X-ray imaging detector CdZnTe the  $\gamma$ -ray group developed. The balloon will be launched in 2001.

The hard X-ray telescope on board InFOC $\mu$ S is almost identical to foil mirror telescope developed for on ASTRO-E, except for focal length being almost doubled to reduce incidence angles. The telescope diameter is 40 cm and the focal length is 8 m, thus angles of grazing incidence are determined as 0.11 to 0.36 deg and the number of nested reflectors is 255.

We designed supermirrors having sensitivity up to 40 keV. After intensive studies, we have chosen a design method called “block method”, where the gradient of periodic length is not continuous but is expressed as a several blocks of constant-period multilayers. The block method has a great advantage of ease to design and flat-top energy response in wide energy range. Detailed discussion is described by Yamashita *et al.* (1998b) and the reference therein.

Flight reflectors are fabricated by Nagoya University and NASA/GSFC. At Nagoya, supermirrors are deposited onto platinum replica foil mirrors made at NASA/GSFC. NASA/GSFC also makes supermirror reflectors by replicating supermirrors directly from mandrel. Nagoya is also making reflectors by “direct replication” for future missions. The rest of this paper is dedicated to characterization of reflectors fabricated at Nagoya University. See Owens *et al.* (2000) on the status of production at NASA/GSFC.

Supermirrors are fabricated by DC magnetron sputtering system. Figure 1 shows a schematics of sputtering target used for supermirror deposition onto platinum replica foils. A target housing has a pair of identical sputtering targets facing to each other. Argon plasma is confined in the cylindrical volume between them, so that plasma does not damage foils. On the other hand, glass mandrel is coated with supermirrors in direct replication process. Target-substrate configuration as shown in figure 1 is used for this purpose. Since glass substrate is more resistive to plasma damage, sputtering target can be faced towards substrate, thus deposition rate can be maximized. See Furuzawa *et al.* (1998) about epoxy replication techniques.

### 3. MEASUREMENT SYSTEM

Fabricated supermirror reflectors were evaluated with hard X-rays at synchrotron radiation facility SPring-8. The experiment is a joint program of Nagoya University and Himeji Institute of Technology. SPring-8 (figure 2) is the world's most powerful third-generation synchrotron radiation facility. Diameter of the SPring-8 storage ring is about 450 m. The gap energy and the maximum current are 8 GeV and 100 mA, respectively. The experiment was carried out at BL24XU (Hyogo Beam Line) Hatch C. X-rays from the Storage Ring (SR) is guided to the hatch through double crystal monochrometer (Si (111)). Energy resolution of the monochrometer ( $E/\Delta E$ ) is about 2500 at 30 keV. The schematics of the experiment setup is shown in figure 3. The X-rays are collimated to  $20 \mu\text{m} \times 20 \mu\text{m}$  size with horizontal and vertical slits. Reflected X-rays are detected with NaI Scintillation counter placed 90 cm away from a sample.

Measured samples were all measured at lower energies (8 and 17 keV) with pencil X-ray beam at Nagoya University in advance to the measurement at SPring-8.

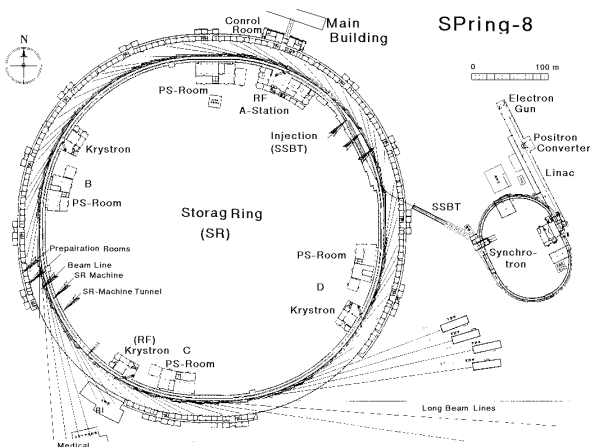


**Figure 2.** The overview of SPring-8 Storage Ring (SR) and accelerators. Diameter of the ring is about 450 m. The gap energy and the maximum current are 8 GeV and 100 mA, respectively.

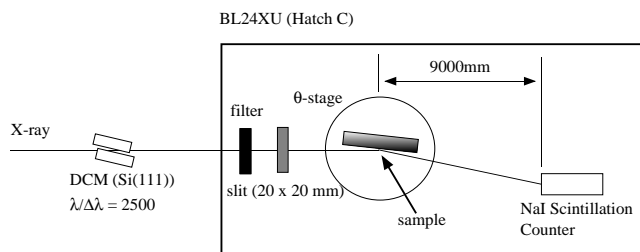


**Figure 3.** Schematics of the experimental setup at SPring-8 BL24XU (Hyogo Beam Line) Hatch C. The monochromatic X-rays are introduced to the Hatch (solid box), and then filtered to reduce beam flux so that sample are not damaged. X-rays are collimated by  $20 \times 20 \mu\text{m}^2$  slit. The flux of incident beam is about  $10^5 \text{ counts s}^{-1}$  depending on the choice of X-ray energy.

### 4. MEASUREMENT RESULTS AND DISCUSSION

#### 4.1. X-ray reflectivity

Four different types of supermirror and multilayers were measured at X-ray energies 25, 30, 35, 45 and 50 keV. The layer structures of these supermirrors are shown in table 1. Figure 4 shows the reflectivity of two types of Pt/C supermirror, 8-block (DESIGN-D) and 7-block (DESIGN-C), fabricated on platinum replica foil mirror. The overlaid model assumes interfacial roughness of 0.35 nm and 0.45 nm (Debye-Waller factor), respectively. The models show good agreements with the data for entire incident angles and photon energies. For the DESIGN-D supermirror, a flat-top and high reflectivity of about 30 % from 0.25 to 0.35 degrees is achieved, which is quite satisfactory for astronomical application. Also the DESIGN-C supermirror has about 30 % reflectivity from 20 to 40 keV at incident angle  $0.295^\circ$ . Figure 5 shows the reflectivity of DESIGN-B supermirrors fabricated by the direct replication method. Interfacial roughness of 0.35 nm was derived from model fitting, which is equivalent to that of supermirrors fabricated of platinum replica mirrors (figures 4). It indicates that we are now successful in replicating supermirrors without distorting layer structures.

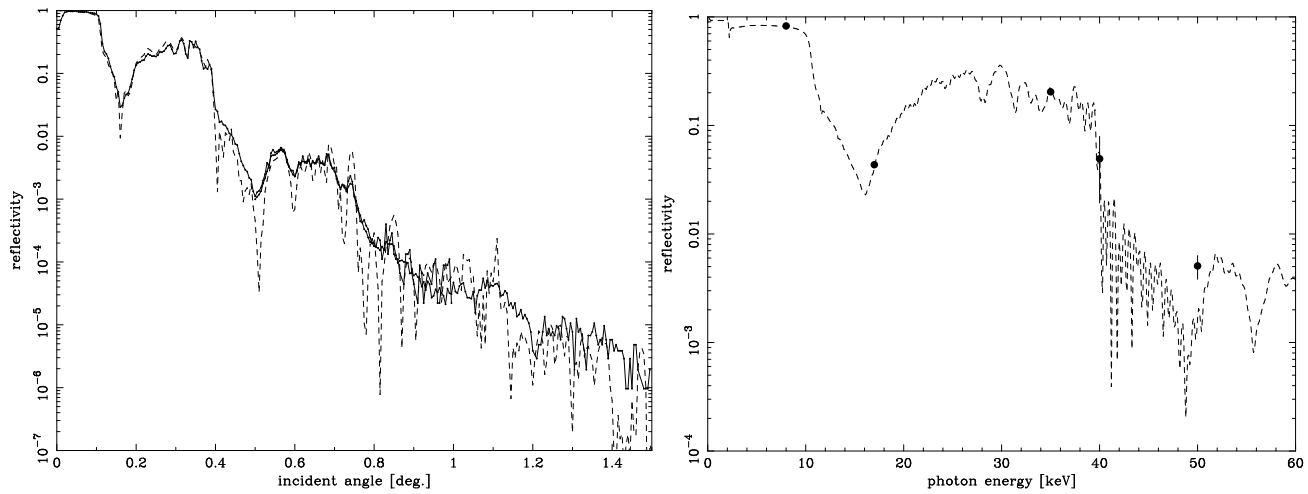


**Figure 4.** Reflectivity of supermirror deposited on platinum replica foil mirror. Left panel: 8-block (DESIGN-D) supermirror measured at 30 keV (solid line). Overlaid model (dashed line) assumes interfacial roughness of 0.35 nm, showing good fit to the data for total reflection and first order Bragg peak complex. The structure of the supermirror is;  $(d(\text{nm}), N) = (5.1, 2)(3.9, 5)(3.6, 3)(3.4, 5)(3.3, 3)(3.2, 7)(3.1, 13)(29, 22)$ .  $\Gamma$  is fixed to 0.4. Right panel: 7-block (DESIGN-C) supermirror measured at incident angle  $0.295^\circ$  (dot with error bars). Overlaid model (dashed line) assumes interfacial roughness of 0.45 nm. The structure of the supermirror is;  $(d(\text{nm}), N) = (5.9, 2)(4.7, 6)(4.4, 4)(3.9, 8)(3.5, 10)(3.2, 14)(3.0, 20)$ .  $\Gamma$  is fixed to 0.4.

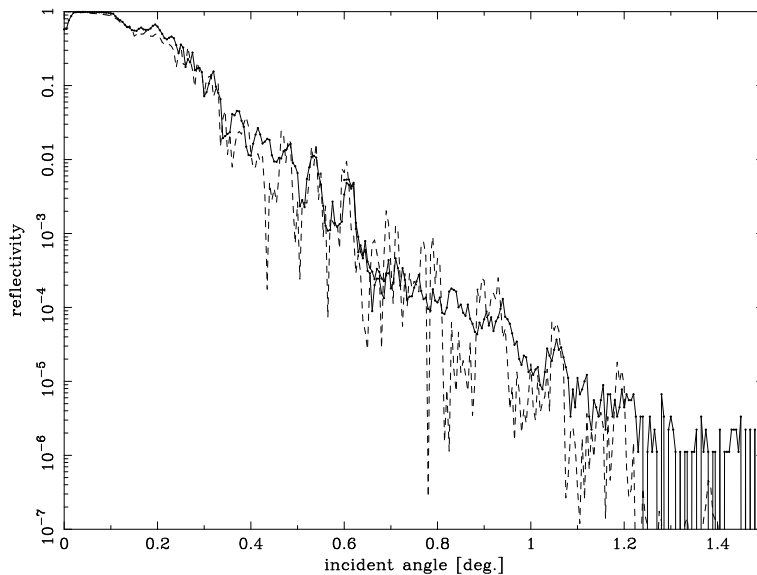


**Figure 5.** Reflectivity of a 6-block (DESIGN-B) supermirror fabricated with direct replication method, measured at 30 keV (solid line). Overlaid model (dashed line) assumes interfacial roughness of 0.35 nm. The structure of the supermirror is;  $(d(\text{nm}), N) = (6.3, 2)(5.6, 3)(5.0, 5)(4.5, 7)(4.0, 10)(3.5, 13)$  with platinum top layer 3.0 nm.  $\Gamma$  is fixed to 0.4.

DESIGN ID	blocks	Pt top coating(nm)	range of $d$ (nm)	total $N$
DESIGN-A	4	–	5.0 – 3.6	44
DESIGN-B	6	3.0	6.3 – 3.5	40
DESIGN-C	7	–	5.9 – 3.0	64
DESIGN-D	8	–	5.1 – 2.9	60

**Table 1.** The design parameters of supermirrors measured at SPring-8.

## 4.2. The reflectivity dependence on a substrate

4-block (DESIGN-A) supermirror was deposited onto different types of substrates, in order to investigate dependency of film quality on substrate. Substrates are platinum replica foil mirror, gold replica foil mirror and float glass. Figure 6 shows the comparison of the reflectivity of supermirrors on 3 substrates. The reflectivity of supermirror on platinum replica foil is higher than that on gold replica foil, even slightly higher than that on a float glass substrate. The purpose of this examination is to see which of platinum and gold replica foil is better substrate for InFOC $\mu$ S mission. Since platinum substrate showed better performance, and turned out to be comparable to or better than glass substrate, we decided to use platinum replica foil mirrors as substrate.

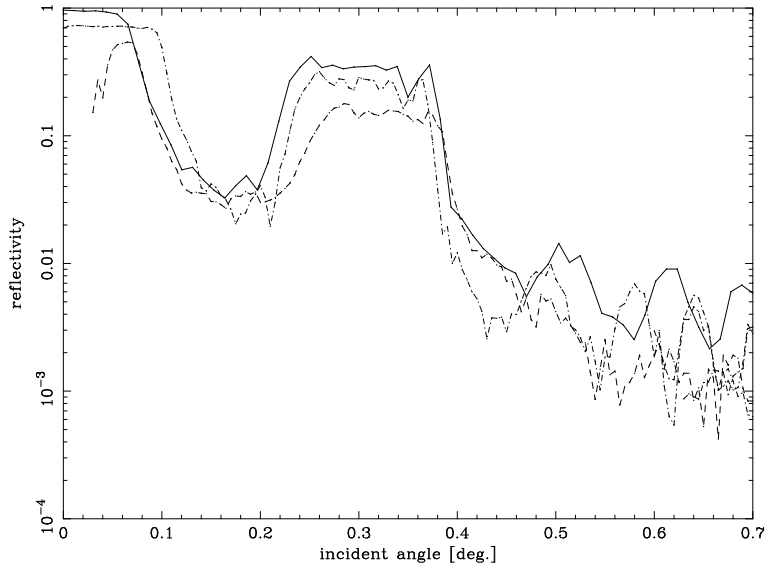


**Figure 6.** Comparison of reflectivity for different substrates, measured at 30 keV. These substrates are float glass (dot-dashed line), gold replica foil (dashed line) and platinum replica foil (solid line). Platinum replica foil is the best one as a substrate. The structure of these supermirror is;  $(d(\text{nm}), N) = (5.0\text{--}4.6, 5)(4.3, 8)(4.0, 13)(3.6, 18)$ .  $\Gamma$  is fixed to 0.4.

## 4.3. X-ray scattering profile

Measurement of hard X-ray scattering profile was carried out to understand surface and interfacial roughness. Scattered tails of multilayers and supermirrors usually show unique structures. This is because of interference between X-rays scattered by geometrical structure into lateral direction, that is, surface roughness, and layered structures into depth direction. The principle of such scattering tails due to the “correlated roughness” is similar to that of multilayer-enhanced reflection gratings. In the case of multilayer gratings, such non-specular enhancement is observed where both of Bragg condition of multilayer and diffraction condition of grating is satisfied.

Figure 7 shows measured distribution of scattered X-rays of multilayer. When the incident angle is slightly off from the Bragg angle, an enhancement is observed in the region of scattered tails. The scattered angle of such non-specular enhancement is where the general form of Bragg condition ( $m\lambda = d(\sin\theta_i + \sin\theta_s)$ ) is satisfied. Note that

$\theta_i$  and  $\theta_s$  are the incident and scattered angle, respectively. Figure 8 shows the same measurement of supermirror. In this case, structure is complexed since periodic length is not constant and multiple enhancements are seen each of which satisfies Bragg condition of corresponding block.

These enhancement may produce significant non-specular power, thus it could contribute to considerable amount of stray lights. Since the principle of non-specular enhancement we have observed is the same as that of multilayer-gratings, we tried to construct the model to describe our measurement based on this principle. Figure 10 shows the modelization in our calculation. The amplitude of surface and interfacial roughness are assumed to be constant for all layer boundaries. Power-law function is adopted as power spectrum density (PSD) of roughness profile, thus we characterized roughness with two parameters; normalization (amplitude) and power-law index.

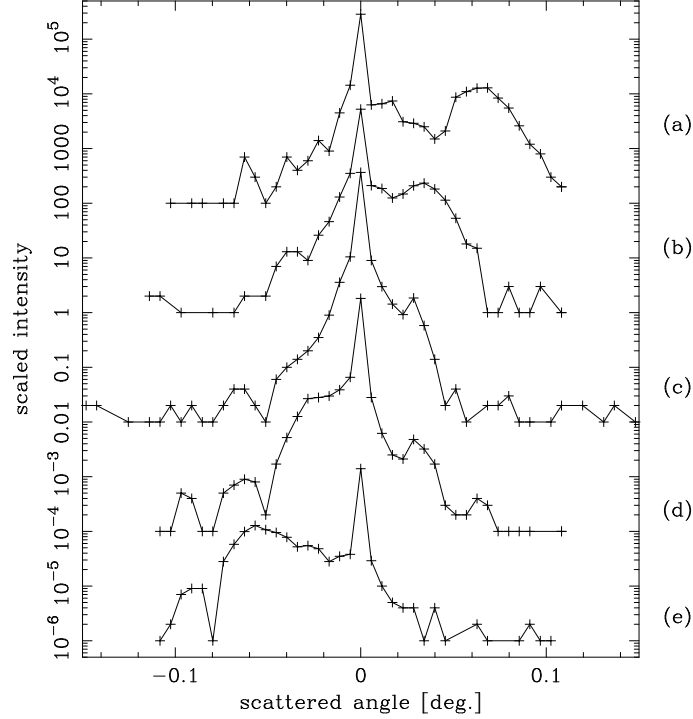


**Figure 7.** Measured scattered tail of multilayer ( $d = 3.76\text{nm}$ ,  $N = 20$ ,  $\Gamma = 0.43$ ) at different incident angle ( $\theta_{in}$ ) near first order Bragg peak. Data was obtained at SPring-8 using monochromatic 32 keV X-rays.  $\theta_{in} = 0.317^\circ$  for first order Bragg peak. The scattered profiles for  $\delta\theta_{in}$  (angle from Bragg peak) =  $-0.032^\circ$ (a),  $-0.017^\circ$ (b),  $0.0^\circ$ (c),  $+0.018^\circ$ (d) and  $+0.028^\circ$ (e).

We estimated PSD of surface and interfacial roughness by measuring scattered X-ray profile of the substrate, that is, the platinum replica foils mirror before multilayer or supermirror is deposited. The scattered profile was measured with 8.0 keV monochromatic X-rays. The PSD was fitted with power-law function with  $\Gamma = 1.0$ . Based on this parameter, we calculated scattered X-ray profile of the sample in figure 8, as seen in the figure 9. As seen from the figure, modelization is quite successful and detailed structure of non-specular enhancements is well represented. Figure 9 is one of the first example, and detailed investigation to fully understand physical conditions of layer boundaries is currently under study.

Non-specular power in scattered tails of supermirrors is suspected to have impact on imaging quality of hard X-ray telescopes. Quantitative study is required, but such impact is expected to be almost negligible. Although non-specular power could be sometimes comparable to specular power, it only appears when incident angle is off-Bragg. Therefore, total reflected power is reduced by the ratio of off-Bragg to on-Bragg reflectivity. Even if non-specular enhancement occupies large fraction of reflected power, it is still smaller than on-Bragg specular power. On the other hand, it is reported that the surface roughness of the top layer is worse than that of substrate from AFM measurement (Namba 1999, private communication).

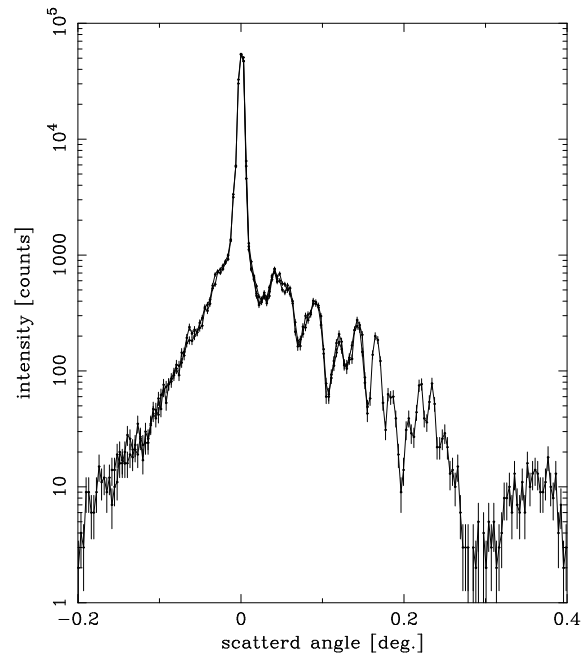


**Figure 8.** The scattered X-ray profile of the same sample as in figure 6 measured at 30 keV. The incident angle is fixed at  $0.221^\circ$ . The enhancement caused by lateral and depth structure is shown in non-specular region.

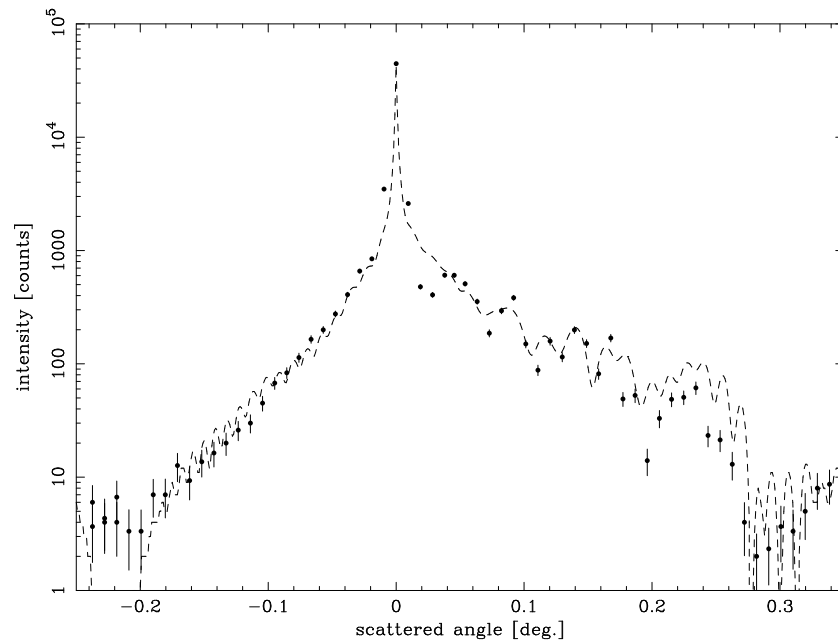


**Figure 9.** Simulated scattered X-ray profile (dashed line) for the sample as in figure 8 (dot with error bars). As a PSD function, power-law function is adopted with  $\Gamma = 1.0$ . The simulated model represents the detailed structure of non-specular enhancement well.

## 5. SUMMARY

Multilayers and supermirrors were fabricated on thin-foil reflector for hard X-ray telescopes. They were evaluated with hard X-rays at SPring-8. Supermirror reflector showed reflectivity of about 30 % for incident angle from 0.25 to 0.35 deg at 30 keV, and its validity for telescope application is proven. Reflectors were also fabricated by direct replication method and showed comparable reflectivity to supermirrors deposited on platinum foil mirror. The profile of scattered tails of multilayers and supermirrors were also measured with hard X-rays. By analogy to multilayer-gratings, we successfully modeled the principle of non-specular power. Based on these experimental results, we are constructing ray-tracing simulation program, in order to generate image and spectral response matrices which are necessary for astronomical observations of celestial objects.

## ACKNOWLEDGMENTS

This work has been supported in part by a Grant-in-Aid for Science Research on Specially Promoted Research, contact No. 07102007, from the Ministry of Education, Science, Sports and Culture, Japan. TO acknowledges the support from the Research Fellowships of the Japan Society for the Promotion of Science.

## REFERENCES

1. Furuzawa, A. *et al.*, 1998, *Proc. SPIE*, **3444**, 576.
2. Owens, S. *et al.*, 2000, *Proc. SPIE*, in press
3. Serlemitsos, P. J. *et al.*, 1995, *Publ. Astron. Soc. Japan*, **47**, 105.
4. Tamura, K. *et al.*, 1998, *Proc. SPIE*, **3448**, 303.
5. Tamura, K. *et al.*, 2000, *Proc. SPIE*, this conference.
6. Tamura, K. *et al.*, 1997, *Proc. SPIE*, **3113**, 285.
7. Yamashita, K. *et al.*, 1998a, *Appl. Opt.*, **37**, 8067.
8. Yamashita, K. *et al.*, 1998b, *J. Synchrotron Rad.*, **5**, 711.